

Searching the Moon for Aluminous Mare Basalts Using Compositional Remote-Sensing Constraints I: Finding the Regions of Interest. *Georgiana Y. Kramer¹, Bradley L. Jolliff², and Clive R. Neal¹

¹ Department of Civil Engineering and Geological Sciences, University of Notre Dame, Notre Dame, IN, ² Department of Earth and Planetary Sciences, Washington University, St. Louis, MO *gkramer@nd.edu

Introduction: The high-Al basalts returned from the Moon are not high in alumina by terrestrial basaltic standards; however, they are characterized by the highest alumina contents of lunar basalts (12 to 15 wt% Al₂O₃). Other key oxide concentrations include MgO=7-12 wt%, FeO=13-17 wt%, TiO₂=1.5-3 wt%, and Th concentrations are 0.1-3 ppm. The high-Al basalts have a relatively narrow range in major element composition, one that can be modeled with simple fractional crystallization. However, Dickinson et al. [1] and Shervais et al. [2] noted the incompatible trace-element concentrations display an eight-fold increase between the lowest and highest abundances, and require a more complex petrogenetic model.

From the work of Papanastassiou & Wasserburg [3], Barnes et al. [4], Compston et al. [5], Nyquist et al. [6], Taylor et al. [7], Dasch et al. [8], Shih & Nyquist [9, 10] and Dasch et al. [11], the high-Al basalt ages of 13 samples returned from the Fra Mauro region by Apollo 14 were found to fall into one of three age groups: 3.9 Ga, 4.1 Ga, and 4.3 Ga. Using isotopic and trace element data, Kramer and Neal [12,13] modeled three distinct melting events of a common source and subsequent assimilation and fractional crystallization (AFC) to produce the high-Al basalts. They also demonstrated that these basalts are true basalts and not impact melts.

In addition to Apollo 14 samples, the Soviet Union Luna 16 mission returned high-Al basalts from Mare Fecunditatis. These basalts differ from the Apollo 14 basalts in their higher TiO₂ content (up to 6 wt%) and greater abundance of light REE compared to their heavy REE. Luna 16 high-Al basalts were also found to be younger than Apollo 14 high-Al basalts, ~3.4 Ga [14]. Apollo 12 also returned one aluminous basalt fragment (12038) that was dated at 3.1 Ga [15].

The old ages of the Apollo 14 aluminous basalt clasts coupled with the fact that they occur as clasts in breccias probably formed by the Imbrium impact suggests that they could be a significant component of ancient basalts that are now buried beneath impact deposits (cryptomare). The existence of younger aluminous basalts in the Apollo 12 samples and at the Luna 16 site suggests that aluminous basaltic volcanism spanned over a billion years. Despite the occurrence of samples within the collection, however, the extent of aluminous basaltic volcanism is poorly known. They are difficult to distinguish owing to (1) burial and disruption of flows that predate some of the large impacts and (2) similarity of their compositions to mixtures of Fe-rich mare basalts and aluminous non-mare materials. In this abstract, we present an approach

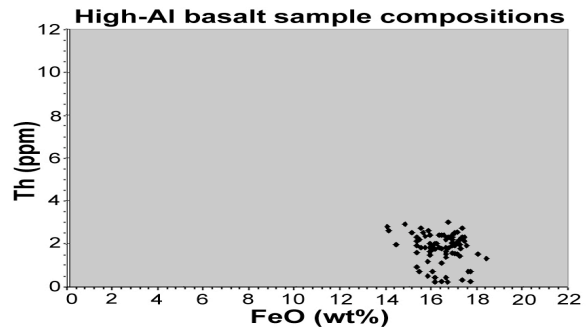


Figure 1a: FeO vs. Th concentrations measured in high-Al basalts (data from clasts in 14321).

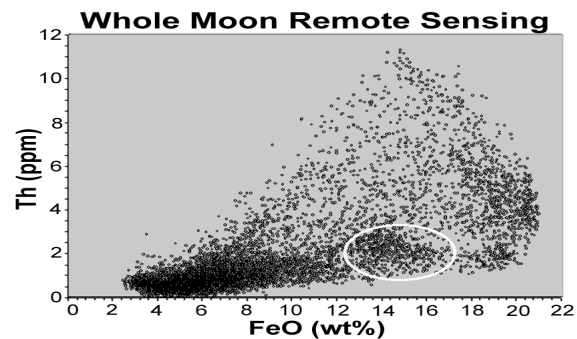


Figure 1b: Region circled depicts the remotely sensed data with FeO and Th in the range of high-Al basalts.

using compositional remote sensing to search for regions that might contain significant amounts of aluminous basalts. In a companion abstract [16], we evaluate several candidate regions.

Remote Sensing for High-Al Basalts: High-Al basalts occupy a specific location in FeO vs. Th compositional space (Fig. 1a). In particular, their FeO concentrations are lower than most high-Fe basalts. Other basalts that plot in this space differ according to their Ti content (VLT basalts and some high-Ti basalts). We note that a plot of global compositions (Fig. 1b) shows a relatively high density of points in the region of intermediate FeO and moderate to low Th (white circle). Although this composition can be obtained by mixing between high-Fe, low-Th basalt and low-Fe-Th nonmare materials, the distribution in Fig. 1b suggests that such mixing is not the only source of the data points in this composition.

For this study we focus on regions where the high-Al basalts would dominate the regolith (e.g., ~70% as the end member). Using Clementine FeO and TiO₂, and Lunar Prospector (LP) thorium, we highlighted areas of the Moon that reflect the

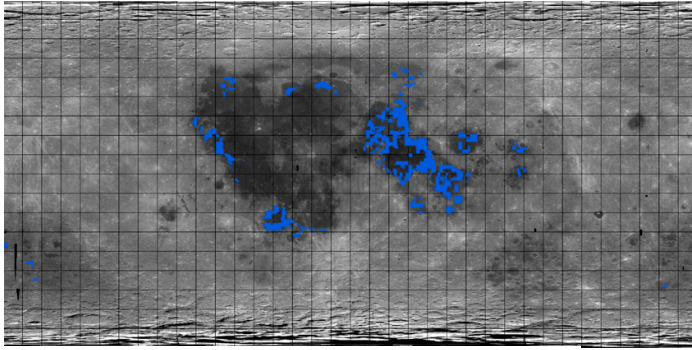


Figure 2: Clementine 750nm base map with blue areas depicting high-Al basalt compositional selection constraints using LP data: FeO=12-18 wt%, TiO₂=1-3.5 wt%, Th=0.1-4ppm.

compositional constraints of the high-Al basalts (Fig. 2). We used as constraints the following ranges: FeO=12-18 wt%, TiO₂=1-3.5 wt%, and Th=0-4 ppm. These ranges exceed the actual ranges for the samples in order to compensate for the effects of mixing of aluminous basalts with other materials in the regolith. Because some differences exist between the Clementine-derived and Lunar-Prospector FeO data sets, we tested constraints using both the LP and Clementine data, and found that they depict similar but not identical regions of interest.

Selected ROIs for HA basalt candidates			
ROI	Clat	Clon	assessment
Maksuto	45S	165W	uncertain
Poincaré	58S	163E	uncertain
W. Proc (Struve)	15N	70W	HA exposure
E. Sinus Roris	45N	63W	uncertain
Humorum	25S	38W	mixing
Pal. Epidemiarum	27S	32W	uncertain
Sinus Iridium	45N	32W	uncertain
N. Imbrium	47N	15W	uncertain
Mare Nectaris	16S	35E	HA exposure
Mare Serenitatis	25N	19E	HA exposure
Mare Tranquillitatis	9N	31E	mixing
Mare Crisium	18N	60E	mixing
Mare Fecunditatis	3S	51E	HA exposure
Mare Marginis	14N	87E	HA exposure
Mare Smythii	2N	89E	HA exposure

Table 1: Fifteen main ROIs distinguished by both Clementine and LP constraints. Center latitude (Clat) and center longitude (Clon) based on Clementine data. Note under assessment these are speculations and not necessarily fact.

Results: As shown in the figure, these constraints highlight 15 main regions of interest (table 1). Each of these regions can be evaluated as potentially representing an area where high-Al basalt is a major component, or as an area where mixing of high-Fe basalt and feldspathic nonmare material has produced the observed compositions. To make this distinction, we evaluate the FeO concentrations of

small craters in each mare region to discern the composition of the underlying lithologic unit and whether these craters are exposing subsurface high-Al basalts. We also compare elemental values for the highlighted regions to the surrounding regions to construct mixing models for each case. This allows the surrounding regions to be interpreted as mixing products (revealed as endmembers) or as a distinct unit. Thus, for example, we interpret the Crisium exposures as mixtures of high-Fe basalts and lower-Fe nonmare materials of the surrounding highlands. Some exposures, however, could be areas where high-Al basalts occur. One such area is Mare Fecunditatis, where Luna 16 samples demonstrate high-Al basalts to be present.

A notable result of this analysis is that there are no extensive exposures of high-Al basalts in the Fra Mauro region. This is not surprising for two reasons: first, the Apollo 14 region and much of the Procellarum KREEP Terrane has Th concentrations that are too high for our constraints. Secondly, the Apollo 14 high-Al basalt clasts occur in ejecta from Imbrium. Any significant high-Al basalt exposed prior to the impact is now likely to be covered by Imbrium proximal ejecta deposits.

Can we distinguish outcrops of high-Al basalt from mare-highland mixtures? Mare Fecunditatis, Mare Nectaris, Mare Smythii, Mare Marginis, areas in northern Imbrium, and the area of western Procellarum near the crater Struve appear to offer the best potential for the occurrence of high-Al basalts, at least at the resolution of the Th data (2 degrees per pixel).

Several of the regions of interest highlighted in Figure 2 are probably not exposures of high-Al basalts. Regolith developed on basin rim basalts undoubtedly reflect the mixing between high-Fe mare basalts and low-Fe highlands. However, those that highlight mare infill, and some of the anomalous areas (i.e. Struve, east of Sinus Roris, Sinus Iridium, etc.) could be real exposures. It is these regions that we analyze further in the companion abstract [16].

References: [1] Dickinson et al. (1985) JGR 90, C365; [2] Shervais et al (1985) JGR 90, C375; [3] Papanastassiou & Wasserburg (1971) EPSL 11, 37; [4] Barnes et al, 1972) GCA 2, 1465; [5] Compston et al (1972) GCA 2, 1487; [6] Nyquist et al (1972) GCA 2, 1515; [7] Taylor et al. (1983) EPSL 66, 33; [8] Dasch et al. (1987) GCA 51, 3241 [9] Shih & Nyquist (1989a) Wksp Moon Transition, 128; [10] Shih & Nyquist (1989b) LPSCXX, 1002; [11] Dasch et al (1991) LPSC XXXII; [12] Kramer & Neal (2003) LPSC XXXIII, [13] Kramer & Neal (2004) in press; [14] Papanastassiou & Wasserburg (1972) EPSL 13, 368, [15] Nyquist et al. (1981) EPSL 55, 335; [16] Kramer et al. (2004), LPSC XXXIV